Bioresource Technology 418 (2025) 131923

Contents lists available at ScienceDirect

Bioresource Technology

journal homepage: www.elsevier.com/locate/biortech

# Stepwise processing of *Chlorella sorokiniana* confers plant biostimulant that reduces mineral fertilizer requirements

Erik Chovancek [a,1], Sylvain Poque [b], Engin Bayram [c], Emren Borhan [a], Martina Jokel [a], Iida-Maria Rantanen [a], Berat Z. Haznedaroglu [c], Kristiina Himanen [b], Sema Sirin [a], Yagut Allahverdiyeva [a,*]

[a] Department of Life Technologies, University of Turku, FI-20014 Turku, Finland
[b] National Plant Phenotyping Infrastructure, Helsinki Institute of Life Science, Biocenter Finland, University of Helsinki, Latokartanonkaari 7, 00790 Helsinki, Finland
[c] Institute of Environmental Sciences, Bogazici University, HKC-318 Hisar Campus, 34342 Bebek, Istanbul, Türkiye

## HIGHLIGHTS

- Stepwise processing rendered algal fractions with various biostimulant activity.
- A blend of fractions enhanced C and N metabolism in tomato plants.
- Application of the blend decreased mineral fertilizer use by 25 %.
- The method results in ample residual biomass for a future biorefinery approach.

## GRAPHICAL ABSTRACT

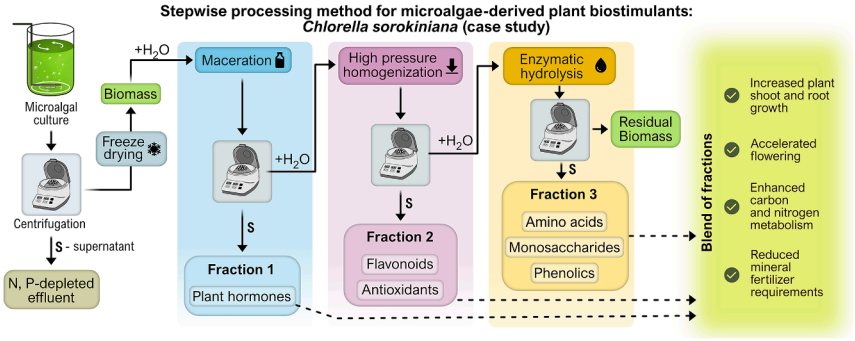


## ARTICLE INFO

*Keywords:*
Microalgae
Maceration
High-pressure homogenization
Enzymatic hydrolysis
Plant phenotyping
Tomato

## ABSTRACT

We developed a stepwise method to transform *Chlorella sorokiniana* microalgal biomass into a potent biostimulant. The method, including maceration, high-pressure homogenization, and enzymatic hydrolysis, preserves the bioactive properties of the biomass as a biostimulant while minimizing plant inhibitory effects. Fractions were characterized individually, and optimal concentrations were determined using a rapid *Arabidopsis* root assay. A blend of optimal concentrations of fractions was identified as the most stimulating extract, increasing the root elongation by 25 %. When applied to tomato plants and monitored using high-throughput plant phenotyping, the blend displayed a 25 % reduction in mineral fertilizer use. Metabolomic analysis of the tomato plants showed significantly enhanced carbon and nitrogen metabolism in the leaves. Our findings indicate that the stepwise processing not only produces an effective biostimulant but also generates substantial residual biomass for a potential multiproduct biorefinery approach that can improve the overall techno-economic outlook.

* Corresponding author.
*E-mail addresses:* erik.chovancek@hhu.de (E. Chovancek), allahve@utu.fi (Y. Allahverdiyeva).
[1] Current address: ; Plant Biochemistry, Heinrich Heine University, Universitätsstr. 1, 40225 Düsseldorf, Germany.

https://doi.org/10.1016/j.biortech.2024.131923
Received 24 August 2024; Received in revised form 30 November 2024; Accepted 30 November 2024
Available online 1 December 2024

## 1. Introduction

Microalgae are photosynthetic microorganisms that efficiently utilize solar energy to capture carbon dioxide and convert it into valuable biomass. Microalgal biomass is an emerging resource for a multitude of products, such as food, feed, pharmaceuticals, cosmetics, nutraceuticals, and other valuable products, replacing fossil-origin chemicals (Premaratne et al., 2022). Despite the growing popularity of microalgae-derived products, commercial algae production systems face challenges due to their complexity and relatively high costs. The techno-economic outlook of algae-based bioproduction can be significantly improved by implementing a targeted downstream design and a multiproduct biorefinery approach, which would produce multiple mid-to-high value by-products and aim for zero waste (Hankamer et al., 2023; Yun et al. 2024).

Among various applications, extracts of different microalgae have demonstrated efficacy as plant biostimulants (Behera et al., 2021). Biostimulants, applied in minute quantities to plants, promote growth, enhance crop yields, improve resistance to abiotic and biotic stresses, and potentially reduce fertilizer dependency (Parmar et al., 2023). The biostimulant market, valued at 2.80 billion USD in 2021, is projected to reach 6.90 billion USD by 2030 with a CAGR of 10.2 % (Verified-Market, 2024). This surge is driven by escalating challenges in crop production due to climate change, soil degradation, and a shift of consumer preferences towards sustainable practices such as organic farming. Currently, microbes, seaweed, and humic substances are widely utilized for the production of biostimulants (Bell et al., 2022).

Microalgae typically contain phytohormones, vitamins, terpenoids, flavonoids, fatty acids, and polysaccharides that can have beneficial effects on plant growth and protection (Ferreira et al., 2023; Kapoore et al., 2021). However, not all microalgae have biostimulant potential, and some extract components display inhibitory effects (Chovanček et al., 2023; Navarro-López et al., 2020). Therefore, selecting suitable algal strains and targeted extraction of bioactive compounds is of high importance for future large-scale productions of plant biostimulants from microalgae. *Chlorella* genus is a globally dispersed genus of the green algae branch (Chlorophyta) that has been widely utilized in human nutrition, aquaculture, animal feed, and cosmetics over the last decades (Abreu et al., 2023).

Unfortunately, the molecular mechanisms underlying plant biostimulants are not well understood. Gaining a clearer understanding of these mechanisms is crucial for developing novel targeted biostimulant formulations tailored to specific crop requirements (du Jardin et al., 2020). This knowledge is essential for improving product efficacy and advancing commercialization efforts. It has been demonstrated that certain microalgal strains can induce the production of terpenoids, phytols, and pyridine-3-carboxamide ($NAD^+$ precursor) in tomato seedlings (Mutale-Joan et al., 2020). It was also shown that extract of *Chlorella vulgaris* leads to an upregulation of citrate synthase and malate dehydrogenase – enzymes crucial to the TCA cycle, phenylalanine pathway, and $NH_4^+$ transformation in lettuce (Puglisi et al. 2022). Other studies have found that extracts from *C. vulgaris* and *Scenedesmus quadricauda* upregulate genes involved in auxin and cytokinin biosynthesis in lettuce, respectively (Santoro et al., 2023). These findings indicate that various compounds, including plant hormones, antioxidants, vitamins, amino acids, or carbohydrates, have the potential to stimulate plant metabolism. To our knowledge, the extraction of multiple bioactive compounds with varying effective concentrations has not been addressed in microalgae. A previous study suggested a cascade system using homogenization and hydrolysis to recover plant biostimulants and lipid retentate (Oancea et al., 2013). However, both extraction methods can be detrimental to the nascent plant growth regulators (Chovanček et al., 2023; Stirk et al., 2020).

In this study, we developed a stepwise processing method to acquire not only soluble compounds (certain plant hormones and vitamins) and macro compound components (amino acids and monosaccharides) but also to mitigate potential risks of plant growth inhibitors (cellular debris) in the extract by decreasing their ratio in the final blend of fractions. We analyzed the fractions produced from *Chlorella sorokiniana* biomass and tested a blend of fractions on tomato plants (*Solanum lycopersicum* L.) using high-throughput plant phenotyping. The results demonstrated that the blend not only enhanced plant growth but also reduced the need for mineral fertilizers by 25 % in tomato greenhouse cultivation. Metabolomic analysis further revealed that the *C. sorokiniana* extract boosted carbohydrate and amino acid metabolism in plant leaves.

## 2. Materials and methods

### 2.1. Algae cultivation and biomass processing

*Chlorella sorokiniana*, strain NIVA-CHL176, was acquired from the Norwegian Culture Collection (NORCCA) and was maintained at room temperature under continuous light (50 μmol photons $m^{-2}$ $s^{-1}$) in Z8 medium. Pre-cultures of algae in a modified BG11 medium were created to imitate wastewater conditions (Azam et al., 2022). After four weeks of pre-cultivation, the inocula were used to prepare 2 L cultures (BG11) with an initial concentration of 0.1 ± 0.05 $gL^{-1}$ ($n = 3$). Each experimental culture was cultivated at 200 μmol photons $m^{-2}$ $s^{-1}$, 21 °C, 14/10 h light–dark cycle, and 1.5 % $CO_2$ (bubbling). The cultures were harvested during the stationary phase (see supplementary materials) by centrifugation (6000 *g*, 15 min, 18 °C; Beckman, USA). The biomass was freeze-dried (74 Pa, −53 °C; Christ, Germany) and stored at −20 °C.

The stepwise biomass processing method comprised the following steps: (i) Maceration involved grinding 750 mg of dried biomass using a mortar and pestle, followed by dissolution in 50 mL of deionized water (MQ; Millipore) with shaking (120 rpm) at 30 °C for three hours (concentration of 15 $g_{DW}L^{-1}$). The supernatant was separated from the pellet by centrifugation (6000 *g*, 10 min, 4 °C) and retained as Fraction 1 (F1). (ii) High-pressure homogenization – the pellet was dissolved in 50 mL MQ by vortexing, and the mixture was processed using a cell disruptor (Constant Systems, UK) by subduing to 275 MPa for a total of five cycles at 4 °C, after which separation by centrifugation followed (6000 g, 30 min, 4 °C). The supernatant was collected and retained as Fraction 2 (F2). (iii) Enzymatic hydrolysis – the pellet was again dissolved with 50 mL MQ and three enzymes (Sigma-Aldrich; Merck Group, USA) were added: cellulase (2 % v/v) from *Aspergillus* sp. (1000 U/g), lipase (2 % v/v) from porcine pancreas (125 U/g), and protease (2 % v/v) from *Bacillus licheniformis* (2.4 U/g). The enzymatic hydrolysis was performed at 37 °C for 24 h. Following this, the mixture was centrifuged again (6000 *g*, 30 min, 4 °C), and the supernatant was collected as Fraction 3 (F3). All fractions were stored at 4 °C, and the final blend was always prepared shortly before application.

### 2.2. Physical, biochemical, and antioxidant characterization of algal extracts

#### 2.2.1. Electrical conductivity

Electrical conductivity (EC) of resuspended biomass and stepwise-processed samples was acquired without temperature compensation, considering the processing time and temperature differences between applications, using an EC meter (LAQUAtwin EC-33; Horiba, Japan).

#### 2.2.2. Total free amino acids

The method of Nielsen et al. (2001) was applied for free amino acid determination in algal extract fractions. Absorbance values were recorded at 340 nm. Serine (0–100 $mgL^{-1}$) was used as the reference standard, and values were expressed as Serine Equivalents (SE) for the concentration of 1 $gL^{-1}$.

#### 2.2.3. Total free monosaccharides

The method of Johnson and Sieburth (1977) was adapted to

determine free monosaccharides in microalgal extracts. Absorbance was measured at 635 nm, and values were calculated for the concentration of 1 $gL^{-1}$.

#### 2.2.4. Total phenolic content

A modified Folin-Ciocalteu method (Chen et al., 2015) was utilized for total phenolic content. Freeze-dried biomass (BM) and the fractions F1 and F2 were diluted to 10 $gL^{-1}$ while F3 to 3 $gL^{-1}$ with pure methanol. Absorbance measurements were recorded at 765 nm. A standard curve for known concentrations of gallic acid was constructed, and data was transformed to gallic acid equivalents (GAE) accordingly. Further calculations for 1 $gL^{-1}$ concentration enabled the comparison of fractions.

#### 2.2.5. Total flavonoid content

The method was described in Kalita et al. (2013). Absorbance was measured at 415 nm relative to a blank (MQ with reaction mixture). Data were transformed according to a standard curve based on known quercetin concentrations (quercetin equivalents; QuE) and calculated for 1 $gL^{-1}$ concentration to facilitate comparison between the different fractions.

#### 2.2.6. Trolox equivalent antioxidant capacity

A modified method by Nowak et al. (2021) was utilized. $ABTS^{+}$ stock solution was prepared freshly. Fractions with a final concentration of 0.1 $gL^{-1}$ were analyzed by recording absorbance at 734 nm. Trolox at a concentration of 25 μM was used as standard. Trolox equivalent antioxidant capacity was calculated as:

$$TEAC = \left[\left(1 - \frac{T}{C}\right) \times 100\right]\%$$

where $T$ and $C$ are the absorbances of the test samples and control reaction, respectively.

#### 2.2.7. DPPH radical scavenging activity

The samples were prepared following the method described by Moyo et al. (2010). Absorbance was measured at 517 nm. Radical scavenging activity was calculated using the formula:

$$RSA = [(1 - (T - E)/C) \times 100]\%$$

where $T$, $E$, and $C$ are the absorbances of the test samples, extract absorbance correction sample, and control (DPPH) reaction, respectively. The results of extracts with a concentration of 0.5 $gL^{-1}$ were compared. Butylated hydroxytoluene (BHT) was the reference standard (79.72 % RSA at 300 $\mu gmL^{-1}$).

#### 2.2.8. Statistical analysis

Total free amino acids and monosaccharides were evaluated for each microalgal culture ($n = 3$) in technical triplicates. Antioxidant assays were performed in several concentrations for each extract targeting optimum absorbance readings (0.2 – 1.0). Statistically significant differences between the mean values were determined using one-way ANOVA followed by Tukey's HSD post hoc test ($p < 0.05$; mean ± SD).

### 2.3. Arabidopsis root elongation assay

The method described in Chovančekˇ et al. (2023) was employed to assess the biostimulant potential of fractions. Briefly, *Arabidopsis thaliana* (Col-0) seeds were sterilized, stratified at 4 °C and cultivated for 5 to 6 days on agar plates (with ½ MS medium) vertically in a growth chamber (120 μmol photons $m^{-2}$ $s^{-1}$, 23 °C, 16/8h). Seedlings of similar root length and size were then transferred to sterile ½ MS plates supplemented with filtered (0.2 μm) extracts of fractions or a blend of fractions and observed for seven days. RGB image analysis of the root length (Image J) on the 7th day was exerted for comparison and stimulation assessment. Three experiments (from each biological replicate of algal culture) for every extract fraction were performed (each with $n = 15$). Statistical analysis was based on ANOVA and Tukey's HSD test for evaluating significant treatment differences ($p < 0.05$, mean ± SE). (Normalized) root stimulation was calculated for each experiment as:

$$RS = [RE/AEC*100]\%$$

where RE is root elongation observed on plate with extract and AEC denotes average root elongation on the control plate.

### 2.4. High throughput plant phenotyping

Tomato seeds, *Solanum lycopersicum* L. cv. Sunvine (BASF, Germany), were stratified at 4 °C in dark on moist filter paper for 48 h before transferring to small pots (350 mL) with peat substrate (VHM620, pH 6.0, R8060; Kekkilä, Finland) in May 2023. On the 13th day after germination (DAG), seedlings were transplanted to bigger pots (3 L) and transferred to the experimental greenhouse of the Finnish National Plant Phenotyping Infrastructure (NaPPI, University of Helsinki, Finland). The seedlings were cultivated in natural light and temperature conditions with abundant watering. Humidifiers were employed to prevent border effects. Commercial fertilizer mix (Calcinit: Kristaflex, 5:3; Yara, Norway) was applied regularly along with automated watering on the 7th, 14th, 21st, 26th, 31st, 35th, and 38th DAG in four levels, 100 %, 75 %, 50 % and 0 % fertigation where 100 % fertigation corresponded to 2 $gL^{-1}$ fertilizer mix application (NPK-100). A blend of fractions [(F1 (0.5 $gL^{-1}$), F2 (0.05 $gL^{-1}$), and F3 (0.05 $gL^{-1}$)] was diluted to the final concentration with 100 mL water and applied manually to assigned pots on the 22nd, 29th, and 36th DAG. Treatment groups were arranged randomly across the greenhouse with ca 1 x 1 m individual space. On the 40th DAG, the third and fourth youngest leaves were collected for metabolic analysis by submerging them into liquid nitrogen and stored at −80 °C. The remaining green parts were harvested and analyzed gravimetrically.

Plant growth was assessed with the automated high-throughput NaPPI phenotyping system (PlantScreen™ Modular System; Photon System Instruments – PSI, Czech Republic) daily from the 21st to 38th DAG (first day and 18th day of imaging, respectively). The system analyzes pixels of images with selected colors (green for leaves and stems; yellow for flowers) using RGB images from top view and multiple side views (Paul et al., 2019). Plant growth was assessed by estimating digital biomass (*DgB*):

$$DgB = \sqrt{SVA^2 \times TVA}$$

where *SVA* is the average area of three side views, and *TVA* is the top view area. The average of *TVA* was used as an estimate of the Projected leaf area (PLA). RGB channel values were extracted and clustered into two color hues: green [85;104;64] and yellow [136;119;24] to assess flowering, using a k-means clustering algorithm implemented in Plantscreen Data Analyser (V.3.2.4.5; PSI, Czech Republic). The proportion of pixels falling into each RGB cluster was computed. A plant was annotated as flowering when the proportion of yellowish pixels exceeded 0.01 % in any of the side view images. Subsequently, the flowering rate was calculated for each treatment over time.

Generalized additive modeling using R (V.4.2.3; R-project) was conducted to fit data by penalized regression splines. The Bayesian credible interval of 95 % was used to distinguish significant differences between treatment groups. In gravimetric analysis, a two-tailed Student's *t*-test was utilized to find significant differences between treated and non-treated plants of each NPK level ($n = 6$).

### 2.5. Liquid chromatography – Mass spectrometry

Tomato leaf samples were prepared using solvent-aided extraction ($n = 6$), as described by French et al. (2018). A pooling strategy was then employed on the extracted samples to create a QC standard. The analysis of extracted samples was carried out on a Q-Exactive Orbitrap LC-HR/

MS system with the Ultimate 3000 UPLC system (Thermo Fisher Scientific, USA) in front-end arrangement (Windarsih et al., 2022). A stepped normalized collision energy was applied for fragmentation in a high-energetic collision cell. The chromatographic separation was conducted on a pentafluorophenyl column (Restek Corp., USA) with a dimension of 150 mm L x 2.1 mm I.D. and 2.7 μm particle size. Compound Discoverer (V.3.3 SP2; CD) platform (Thermo Fisher Scientific, USA) was utilized for the database search, annotation, and MS/MS data visualization. The spectra were aligned by retention time using ChromAlign algorithm. Trace Finder (V.4.1) data visualization platform (Thermo Fisher Scientific, USA) was utilized to create a targeted screening method for CD-detected compounds. The relative standard deviation (RSD) was calculated for the following peak variables: area, height, and retention time. The acceptance criterion was RSD $< 30$ %.

Statistical analysis was performed on the CD platform. The *p-value* of the per-group ratio was calculated using a two-tailed Student's *t*-test with Benjamini-Hochberg correction for false discovery rate. Principal component analysis, differential analysis with fold change (FC) and volcano test, and hierarchical clustering were also conducted with CD. For functional analysis of afflicted pathways, the mummichog algorithm was executed using the MetaboAnalyst (V.6.0) platform. The same platform was employed to conduct data mining utilizing the KEGG network library search function.

### 2.6. Biopesticide properties

The biopesticide efficacy of the fractions was evaluated using a plant pathogenic oomycete *Phytophthora cactorum* (MUCL 213), employing the *in vitro* antimicrobial test on plates as described in Jokel et al. (2023). The oomycete *P. cactorum* was obtained from the Belgian Coordinated Collections of Microorganisms (BCCM). Three working concentrations (7.5 $gL^{-1}$, 15 $gL^{-1}$, and 22.5 $gL^{-1}$) of all fractions were prepared with sterile MQ, and a 100 μL aliquot was applied to the surface of potato dextrose agar (Scharlau, Spain) plates containing 200 mL $L^{-1}$ tomato juice. To compare the effectiveness of the fractions, crude microalgae extract with the same biomass and concentration was prepared by three cycles of freeze-thawing. Sterile MQ served as the control. A small mycelial disk was positioned at the center of each plate, and the plates were incubated for seven days at 25 °C. All treatments were executed in triplicates ($n = 3$). Assessment of growth inhibition was performed by measuring the diameter of the *P. cactorum* growth in the treated plates relative to the control plates. Statistical analysis was based on ANOVA and Tukey's HSD test for evaluating significant differences between fractions ($p < 0.05$, mean ± SD).

## 3. Results and Discussion

### 3.1. Impact of stepwise biomass processing on physical, biochemical, and antioxidant properties of the C. Sorokiniana extract fractions

We have designed a stepwise extraction method for processing *C. sorokiniana* biomass, which included maceration (F1), homogenization (F2), and enzymatic hydrolysis (F3). We first evaluated the dried biomass of *C. sorokiniana* and the three fractions (F1-F3) by measuring their electrical conductivity (Table 1). Electrical conductivity (EC) serves as an indicator of cell breakage and the release of the ionic intracellular components into the extract (Carullo et al., 2022). Based on the measured values, it can be inferred that the maceration step (F1) increased ion release by 38 % compared to dry biomass. However, only a small fraction of ions were released into the water after applying high-pressure homogenization to the residue (F2). Following enzymatic hydrolysis, EC substantially increased about seven-fold, reaching up to 2.8 $mScm^{-1}$. Various compounds, such as carboxylic acids (also certain plant hormones), amino acids, polyols, and phenolics, are polar in character and can contribute to the electrical conductivity of the extracts. Therefore, the increase in EC in F1 and F3, where the release of these compounds is expected, is not surprising. These results suggest that maceration and enzymatic hydrolysis are highly efficient in releasing ionic forms into the extract, while high-pressure homogenization applied after the removal of free ions by maceration cannot provide satisfactory release of these forms into the extract.

**Table 1**
Electrical conductivity after each step of biomass processing ($n = 3$).

| EC # | Fraction | Characteristics | Mean ± SD ($\mu S.cm^{-1}$) |
|---|---|---|---|
| EC 0 | | Dried biomass + water (15 $gL^{-1}$) | 385.0 ± 14.4 |
| EC 1 | F1 | Macerate (30 °C, 120 rpm, 3 h) | 530.7 ± 63.1 |
| EC 2 | F2 | Homogenate (275 MPa, 5 cycles) | 149.0 ± 36.5 |
| EC 3 | F3 | Lysate (enzymes*, 2 % v/v each) | 2840.0 ± 141.1 |

* cellulase (*Aspergillus* sp.), lipase (porcine pancreas), protease (*Bacillus licheniformis*).

The fractions were further characterized for total free amino acids (TAA), total free monosaccharides (TMS), total phenolic content (TPC), total flavonoid content (TFC), and potential antioxidant activity by TEAC and DPPH radical scavenging assays (Fig. 1). As expected, TAA and TMS increased exponentially in F3, reaching the highest values observed in the experiment (Fig. 1a, 1b). TPC exhibited a similar trend, with F3 reaching an equivalent of 23.7 ± 1.2 μg gallic acid $mL^{-1}$ (Fig. 1c). It is important to note that the Folin-Ciocalteu reagent, used in this method, reacts not only with phenolics but also with a broad range of antioxidants. Consequently, TPC serves as an approximation of total antioxidant content. This could also account for the higher TPC values observed in F3 than BM. TFC results, on the other hand, indicated that the highest flavonoid content, an equivalent of 3.4 ± 0.2 μg quercetin $mL^{-1}$, was found in F2, nearly matching the TFC of the freeze-dried biomass (Fig. 1d). In the TEAC assay, F3 attained the highest antioxidant capacity at 45.3 ± 5.5 % of Trolox activity, followed by BM at 30.4 %, while F1 and F2 displayed activity ranging from 8.7 % to 11.3 % (Fig. 1e). DPPH radical scavenging activity was highest in F2 with 19.3 ± 0.1 %, tightly followed by the other two fractions (Fig. 1f). F1 showed the lowest antioxidant potential amongst the fractions in all performed tests. The results also indicate that although F3 had the highest concentrations of free amino acids and monosaccharides, both F2 and F3 were rich in valuable plant-stimulating compounds, including antioxidants with varying radical scavenging capacities (ABTS, DPPH).

### 3.2. Assessment of biostimulant potential of fractions and their blend using Arabidopsis root elongation assay

Next, we evaluated the plant-stimulatory effects of each fraction and their blend by measuring root elongation in *A. thaliana* seedlings grown on agar plates in sterile conditions. We tested various concentrations for each fraction – F2 and F3 exhibited inhibition at concentrations above 0.05 $gL^{-1}$, while F1 was most effective at concentrations of 0.3 and 0.5 $gL^{-1}$ (data not displayed). Therefore, we compared F1 at 0.3 $gL^{-1}$ with F2 and F3 at 0.05 $gL^{-1}$. At these concentrations, all fractions enhanced root elongation of the seedlings (Fig. 2a). Specifically, F1 and F3 increased primary root growth by 14.2 % and 16.5 %, respectively, while F2 showed only 11 % increase (Fig. 2b). A combined blend of all the fractions at the aforementioned concentrations resulted in 25 % increase in root elongation compared to control seedlings grown on half-strength MS media. The level of root stimulation is considerably higher than previous findings, where single-step extractions from dried *C. sorokiniana* biomass only led to root elongation increases of 6 % and 7 % for bead-milling and acid hydrolysis, respectively (Chovanček et al., 2023).

Macerates of algal biomass have been shown to contain plant hormones that effectively stimulate the germination of various crops (Ferreira et al., 2023). However, their effectiveness in promoting growth during later vegetative stages is generally lower and often unsatisfactory (Stirk et al., 2020). On the other hand, plant biomass hydrolysates are

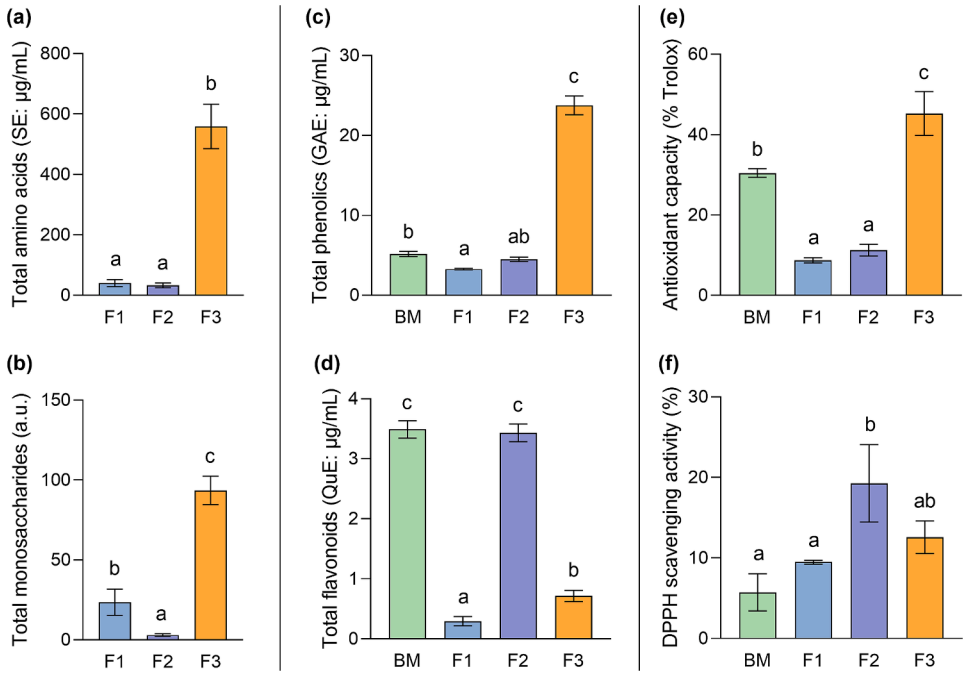


**Fig. 1.** Biochemical properties and antioxidant activity of *C. sorokiniana* resuspended dried biomass (BM) and the three fractions (F1 – F3).Results were compared for the following concentrations: 1 $gL^{-1}$ (a – d); 0.1 $gL^{-1}$ (e); 0.5 $gL^{-1}$ (f). Values are expressed in equivalents of (a) serine (SE), (b) arbitrary units (a.u.), (c) gallic acid (GAE), (d) quercetin (QuE), (e) trolox, (f) % (standard: butylated hydroxytoluene). Bars represent mean ± SD ($n = 3$). Letters above bars indicate significant differences according to Tukey's multiple comparison test (ANOVA, $p < 0.05$).

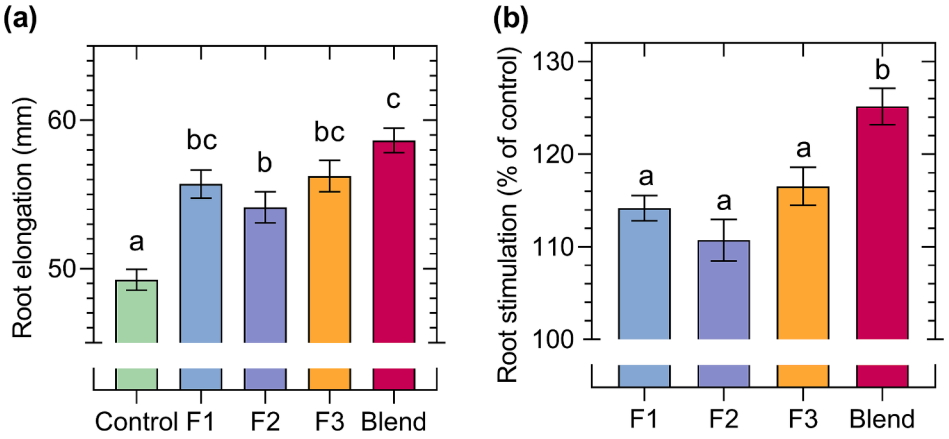


**Fig. 2.** *A. thaliana* root elongation as an indicator of plant biostimulant potential of the fractions (F1 – F3) and blend of fractions. A. *thaliana* seedlings were transferred to ½ MS media (control) supplemented with 0.3 $gL^{-1}$ (F1) or 0.05 $gL^{-1}$ (F2 and F3), and their blend consisting of F1 (0.3 $gL^{-1}$), F2 (0.05 $gL^{-1}$), and F3 (0.05 $gL^{-1}$). Root elongation on the 7th day after transfer (a). Bars represent mean ± SE ($n = 27 – 85$). Root stimulation is expressed as % of stimulation compared to the control mean of each experiment (b). Letters above bars indicate significant differences according to Tukey's multiple comparison test (ANOVA; $p < 0.05$).

widely recognized as plant biostimulants due to their high amino acid content (Paul et al., 2019). However, hydrolysis and mechanical processing of algal biomass can lead to the degradation or radicalization of bioactive compounds, resulting in reduced plant stimulation or even inhibition (Stirk et al., 2020; Chovanček et al., 2023). The sequential extraction of biomass, as presented here, allowed a selective extraction of the chemically sensitive compounds present in F1, and reduction of F3, which was rich in amino acids and monosaccharides and therefore required a lower effective concentration. F2 showed the highest flavonoid content and displayed root stimulation at low concentrations and was therefore also included in the final blend of fractions. The cell rupture after the applied high-pressure homogenization was visually confirmed with microscopy (data not displayed). High-pressure homogenization facilitates cell disintegration and extraction of carbohydrates, proteins, and lipids from microalgal biomass (Carullo et al., 2022). As a result, high amounts of intracellular compounds, e.g., peptides, enzymes, pigments, and residual components, are released into the extract. Some of these compounds, such as flavonoids, play a key role in plant defense (Ramaroson et al., 2022). However, most of the residual components after homogenization are plausibly large in size and not accessible for plants and might contribute to clogging of plant root pores leading to water shortage in the intercellular space. High organic material content and low volumetric requirements in the final blend make F2 a promising resource for use in a biorefinery concept. Further analysis of the composition of F2 could provide valuable insights into its contribution to the final blend's stimulation efficiency and its potential application in other products.

### 3.3. High throughput plant phenotyping to study crop stimulation

To evaluate the crop stimulation potential, we applied a blend of fractions (0.5 $gL^{-1}$ F1, 0.05 $gL^{-1}$ F2, and 0.05 $gL^{-1}$ F3) to tomato seedlings in pots, providing the treatment three times during a period of 18 days. During this time, plant growth was monitored with high-throughput RGB imaging. The experimental design included four levels of fertigation, NPK 100 %, 75 %, 50 %, and 0 %, to evaluate how the microalgal extract might enhance growth and reduce fertilizer usage. Plant growth and overall fitness were evaluated through digital imaging parameters (Fig. 3) and gravimetric analyses (see supplementary materials). Digital biomass (DgB) was measured using images from four perspectives (top and three side views) to accurately calculate plant (green) biomass (Thoday-Kennedy et al., 2021). Fig. 3a shows a gradual increase of DgB across the sample spectrum, with a notable bifurcation observed in the NPK-75 subgroup towards the end of the experiment. Therefore, we focused on the NPK-75 subgroup for more detailed analyses. Fig. 3b highlights a significant growth increase in the extract (BS)-treated plants between the fourth and the sixth day. Additionally, the projected leaf area (PLA), derived from top-view camera images, further corroborates the observed growth stimulation, confirming a marked increase in plant growth during the final days of the experiment (Fig. 3c). PLA is closely related to the leaf area index (LAI), which measures the efficiency of a plant's leaf area in capturing light. LAI is often used to evaluate vegetation efficiency and productivity in an ecological context (Tripathi et al., 2018). Further analysis of RGB images also allowed us to evaluate the flowering rate by quantifying the yellow pixels of the flower petals. A notable acceleration in flowering was observed in the BS-treated group between days 10 and 15 (Fig. 3d). Additionally, the fresh weight of shoots significantly increased from 193.6 ± 1.6 g to 201.6 ± 3.1 g ($p < 0.05$, *t*-test), matching the weight of those receiving NPK-100 without BS treatment (Fig. 3e). In fact, there was a slight increase in all fertilizer levels except for NPK-0. Except for NPK-0, the total fresh weight of (unripened) tomato fruits per plant increased in all other NPK subgroups treated with the BS, although the results were statistically not significant (Fig. 3f). The NPK-0 group, being deficient in essential nutrients, likely experienced accelerated senescence, and earlier fruiting (Sakuraba, 2022).

In summary, the blend of *C. sorokiniana* biomass fractions produced optimal results when used in conjunction with fertigation at 75 % of the recommended concentration. This combination achieved growth similar to that of plants receiving 100 % NPK, effectively saving 25 % of mineral fertilizer while using very low concentrations of the fractions' blend. Conversely, the addition of the biostimulant to NPK-0 did not result in any observable growth improvement. This finding supports the essential assumption that our extract functions as a biostimulant rather than a fertilizer. It is conceivable that the applied extract promotes the proliferation of plant growth-promoting microorganisms naturally present in the soil. Previous research has indicated that direct application of *C. sorokiniana* biomass positively affects the soil microbiome during barley cultivation, though no direct plant stimulation was observed (Suleiman et al., 2020). Although we cannot rule out an effect on plant growth-promoting microorganisms on the tomato plants, the observed root stimulation in *Arabidopsis* seedlings grown under sterile conditions (Fig. 2) suggests a direct effect on plants.

### 3.4. Metabolome of the stimulated tomato plants

To understand the integral effects of the stepwise processed microalgal biostimulant on plants, we next performed a metabolome analysis

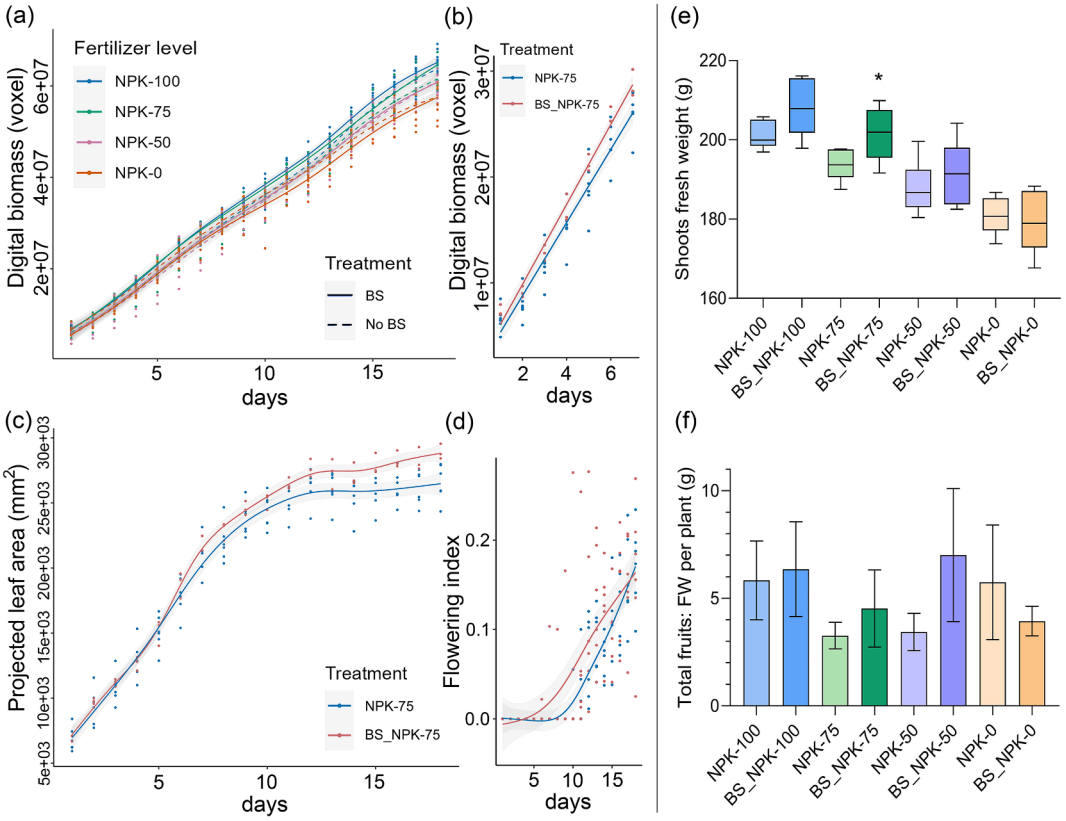


**Fig. 3.** Tomato plant stimulation by the *C. sorokiniana* blend of fractions. Four levels of mineral fertilizer (NPK) were used – 100 %, 75 %, 50 %, and 0 % (NPK-100, NPK-75, NPK-50, NPK-25, and NPK-0). Generalized additive modeling was utilized to assess parameters acquired from plant imaging (a – d). Means of biostimulant-treated (BS) and non-treated (No BS) plants are indicated with continuous and dashed lines, respectively (a). Points represent single values; grey shaded region represents the 95 % Bayesian credible interval. Days – days of imaging. Bars in (e) represent the interquartile range (and median), and the full sample range is depicted with error bars. Columns in (f) represent mean ± SE ($n = 6$). Asterisk denotes significant difference according to Student's *t*-test (BS vs respective control).

of the extract-treated tomato plants. Although various bioactive compounds have been identified in algae, current knowledge of molecular mechanisms responsible for plant stimulation by microalgal products remains limited, which can be attributed largely to the synergistic effects of several algal components (Gemin et al., 2019). In this study, we analyzed the metabolome of tomato plants in the NPK-75 fertilizer group, comparing non-treated (No BS) versus treated (BS) plants. Out of 2261 distinct *m/z* values, altogether, 987 were annotated employing CheBi, KEGG, FoodDB, HMDB, and MassBank databases. Statistical analysis of $\log_2$ FC ($\alpha = 0.05$), grouped by samples (3rd and 4th youngest leaves), revealed a total of 115 differentially abundant metabolites (DAM), out of which 50 metabolites were annotated. Differential analysis showed that 19 annotated metabolites are significantly reduced or elevated in the tomato plants treated with the microalgal extract (Fig. 4a). Fig. 4b displays the DAM and hierarchical clustering with scaling based on sample $\log_2$ FC results. Additionally, functional analysis based on the mummichog algorithm identified seven pathways that harbored 33 metabolite hits.

Data mining of the annotated DAM revealed several links between end products and metabolite precursors (Fig. 4c). The metabolite with the highest fold change was *cis*-zeatin-7-N-glucoside, indicating an increased level of cytokinins in the BS-treated plants (Table 2). Zeatins are produced in the terpenoid-quinone pathway via shikimate (Tong, 2013), which was also elevated. This pathway branches from the phosphoenolpyruvate pathway, which begins at 2-P-glycerate, a metabolite that was also elevated, suggesting a direct link to carbohydrate metabolism (Tzin and Galili, 2010). Additionally, the phenylpropanoid pathway, which utilizes shikimate as a precursor and is responsible for flavonoid production (Liu et al., 2021), showed the highest number of hits in the functional analysis. Although the differential analysis did not reveal any change in specific flavonoids, the mummichog algorithm identified several relevant hits, including derivatives of sinapic acid, coniferyl alcohol, and coumarins (see supplementary materials). Interestingly, phenylacetic acid, an intermediate between the two pathways favoring the terpenoids, showed reduced accumulation in the study. Additionally, uridine 5′-diphosphate (UDP), a by-product of *cis*-zeatin-7-N-glucoside production, was found to be elevated in the treated plants. UDP is a precursor to UTP, which is utilized either in protein synthesis or released and reused in the pyrimidine/amino acid metabolism (Zhang et al., 2020).

In the amino acid metabolism, L-glutamate, purines, adenine, and adenosine were significantly elevated, while L-threonine was reduced. Adenine contributes directly to protein biosynthesis and serves as a precursor to adenosine. Adenosine, in turn, is a precursor in ATP metabolism, the energetic center of cells. It also plays a role in producing cAMP, a signaling molecule important in sensing environmental stresses (Blanco et al., 2020). Both adenine and adenosine were increased in the study.

The glycine-serine-threonine pathway plays a central role in various metabolic processes, including gluconeogenesis, porphyrin biosynthesis, and glycerophospholipid metabolism (Mouillon et al., 1999; Neuberger, 1980). The latter can produce glycerophosphocholine, a metabolite involved in membrane remodeling (van der Rest et al., 2002), which was found to be decreased in this study. On the other hand, phytosphingosine, which is involved in membrane biosynthesis and transport, was significantly increased through the acetylhomoserine pathway. A list of all annotated DAM, their fold changes, and key biological roles are displayed in Table 2.

Although further research is required to gain greater insights into the intricate mechanisms of interaction between biostimulants and plants,

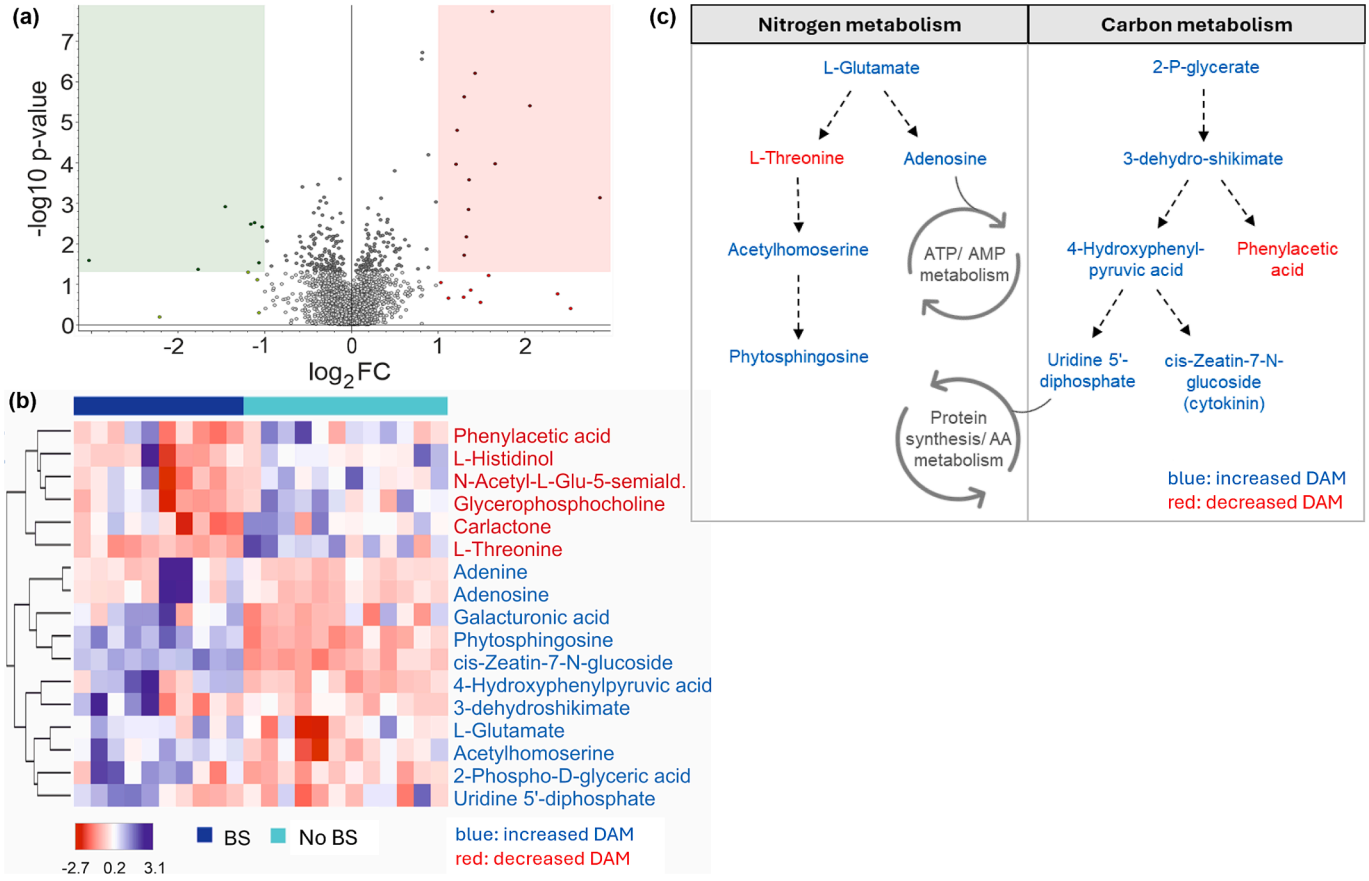


**Fig. 4.** LC-MS results of the NPK-75 biostimulant-treated (BS) versus non-treated (No BS) tomato plant samples. Volcano plot with $\log_2$ FC of all annotated features (a). Heatmap of differentially abundant metabolites (DAM) with respective $\log_2$ FC values (b). Afflicted pathways in tomato plan (c).

**Table 2**
Differentially abundant metabolites (DAM) in the biostimulant-treated tomato plants of the NPK 75 % fertilizer level ($n = 6$; $p < 0.05$).

| Class | Metabolite | log2 FC | p-value | Regulation |
|---|---|---|---|---|
| Amino acids & derivatives | L-Glutamate | 0.62 | 3.017E-02 | up |
| | Acetylhomoserine | 0.38 | 2.023E-02 | up |
| | L-Histidinol | −0.27 | 3.108E-04 | down |
| | N-Acetyl-L-glutamate 5-semialdehyde | −0.28 | 4.098E-02 | down |
| | L-Threonine | −0.35 | 1.307E-02 | down |
| Hormonal precursors | *cis*-Zeatin-7-N-glucoside | 1.41 | 8.270E-09 | up |
| | Carlactone | −0.56 | 7.080E-03 | down |
| | Phenylacetic acid | −0.57 | 9.552E-03 | down |
| Lipids & derivatives | Phytosphingosine | 1.14 | 6.800E-06 | up |
| | Glycerophosphocholine | −0.24 | 4.136E-02 | down |
| Nucleotide derivatives | Adenine | 1.24 | 2.525E-02 | up |
| | Adenosine | 1.19 | 4.182E-02 | up |
| | Uridine 5′-diphosphate | 0.29 | 1.334E-02 | up |
| Secondary metabolite precursors | 2-Phospho-D-glyceric acid | 0.71 | 2.370E-02 | up |
| | Galacturonic acid | 0.55 | 3.615E-02 | up |
| | 3-dehydroshikimate | 0.34 | 5.383E-03 | up |
| | 4-Hydroxyphenylpyruvic acid | 0.17 | 5.079E-03 | up |

the modulation of the carbon and nitrogen metabolism can be linked to the application of algal extract. It should be noted that the plants compared were not affected by nutrient depletion, and metabolome analysis focused on long-term metabolic changes rather than the immediate effects following biostimulant application.

### 3.5. Multiproduct biorefinery potential

The economic value of the extraction could be further enhanced by developing additional valuable products from the extract. Previous experiments have shown that extracts of *C. sorokiniana* can inhibit the growth of the plant pathogenic oomycete *Phytophthora cactorum* (Jokel et al., 2023). To investigate this potential, we compared the fractions to a crude extract obtained from the same *C. sorokiniana* biomass using three cycles of freeze-thawing. However, none of the fractions exhibited an antimicrobial activity against *P. cactorum* (see supplementary materials). Only the freeze-thawed biomass extracts displayed growth inhibition of *P. cactorum* of 53.5 % at 15 $gL^{-1}$, consistent with previous findings (Jokel et al., 2023). Inhibition of *P. cactorum* growth drastically decreased to 39.4 % at 7.5 $gL^{-1}$, while a higher concentration of 22.5 $gL^{-1}$ resulted in 76.8 % inhibition. This shows a clear concentration-dependent effect of the freeze-thawed extract on oomycete. Although the overall results indicate that the described stepwise extraction method is not suitable for biopesticide formulation, it confirms that *C. sorokiniana* biomass still retains antimicrobial activity. More research is needed to develop extraction methods for formulations that combine both biostimulant and biopesticide properties.

The stepwise processing method also presents opportunities to enhance the extraction potential. Since water was used as the solvent in all extraction steps, the residual biomass, up to 45 % of the original biomass (data not displayed), likely contains valuable hydrophobic elements, e.g., fatty acids. Fraction 2, which showed less biostimulant potential, could be along with the residual biomass redirected towards other products (e.g., hydrolysates, chars, biofuels). Although further tests and large-scale experiments are required for a rigorous techno-economic assessment, it is conceivable that a biorefinery approach with broader utilization pathways for residual biomass, where nearly half of the microalgal biomass is retained for its original purpose (e.g. aquafeed), could present a competitive alternative to the conventional utilization approach. In large-scale production, using sedimentation instead of centrifugation, and exploring alternatives to high-pressure homogenization, such as microwaves, ultrasound, or pulse-field techniques, could reduce production costs (Kapoore et al., 2021). Additional research is needed to advance this proof of concept into an economically viable technology for producing high-quality novel agrichemicals at an affordable price at large scale.

## 4. Conclusions

Stepwise processing of *Chlorella sorokiniana* biomass rendered fractions with notable biostimulant potential. Fractionation reduced nascent inhibitors in a blend of fractions that contained micro- and macronutrients, hormones and antioxidants. The blend, composed of optimized concentrations of fractions, enhanced growth, flowering, and fruiting of tomato plants while reducing fertilizer use by 25 % compared to standard practices, indicating its role in promoting the plants‘ innate anabolic processes. The stepwise fractionation process generated a substantial amount of residual biomass (about 45 %), creating opportunities for future multiproduct biorefinery approaches that could significantly improve the techno-economic outlook.

## CRediT authorship contribution statement

**Erik Chovancek:** Writing – review & editing, Writing – original draft, Visualization, Validation, Software, Methodology, Investigation, Formal analysis, Data curation, Conceptualization. **Sylvain Poque:** Writing – review & editing, Visualization, Validation, Software, Methodology, Investigation, Formal analysis, Data curation. **Engin Bayram:** Writing – review & editing, Visualization, Validation, Software, Methodology, Investigation, Formal analysis, Data curation. **Emren Borhan:** Writing – review & editing, Validation, Investigation, Formal analysis, Data curation. **Martina Jokel:** Writing – review & editing, Validation, Investigation, Formal analysis, Data curation. **Iida-Maria Rantanen:** Writing – review & editing, Validation, Investigation. **Berat Z. Haznedaroglu:** Writing – review & editing, Resources. **Kristiina Himanen:** Writing – review & editing, Resources. **Sema Sirin:** Writing – review & editing, Project administration, Methodology, Conceptualization. **Yagut Allahverdiyeva:** Writing – review & editing, Resources, Project administration, Funding acquisition, Conceptualization.

## Declaration of competing interest

The authors declare that they have no known competing financial interests or personal relationships that could have appeared to influence the work reported in this paper.

## Acknowledgements

This study was financially supported by the European Union Horizon Europe IA project REALM (Grant Number: 101060991), the Tandem Industry Academia project - AgriAlga (grant number #373), and the NordForsk Nordic Center of Excellence ‘NordAqua’ (Grant Number: 82845). The authors would like to thank HELLE Oy for kindly providing tomato seeds. We also thank Tapio Ronkainen and Joni Vuorinen for their assistance with preparing and conducting microalgal cultivation.

## Appendix A. Supplementary data

Supplementary data to this article can be found online at https://doi.org/10.1016/j.biortech.2024.131923.

## Data availability

The data that support the findings of the study are openly available at:

http://hdl.handle.net/11304/9b80c8e0-871c-4720-ba57-d19978a6b8bf.

## References


Abreu, A.P., Martins, R., Nunes, J., 2023. Emerging Applications of *Chlorella* sp. and Spirulina (*Arthrospira*) sp. *Bioengineering* 10 (8), 955. https://doi.org/10.3390/bioengineering10080955.

Azam, R., Kothari, R., Singh, H.M., Ahmad, S., Sari, A., Tyagi, V.V., 2022. Cultivation of two *Chlorella* species in open sewage contaminated channel wastewater for biomass and biochemical profiles: comparative lab-scale approach. *J. of Biotechnol.* 344, 24–31. https://doi.org/10.1016/j.jbiotec.2021.11.006.

Behera, B., Supraja, K.V., Paramasivan, B., 2021. Integrated microalgal biorefinery for the production and application of biostimulants in circular bioeconomy. *Bioresour. Technol.* 339, 125588. https://doi.org/10.1016/j.biortech.2021.125588.

Bell, J.C., Bound, S.A., Buntain, M., 2022. Biostimulants in agricultural and horticultural production. *Horticult. Rev.* 49, 35–95. https://doi.org/10.1002/9781119851981.ch2.

Blanco, E., Fortunato, S., Viggiano, L., de Pinto, M.C., 2020. Cyclic AMP: A polyhedral signalling molecule in plants. *Int. J. of Mol. Sci.* 21, 4862. https://doi.org/10.3390/ijms21144862.

Carullo, D., Abera, B.D., Scognamiglio, M., Donsì, F., Ferrari, G., Pataro, G., 2022. Application of pulsed electric fields and high-pressure homogenization in biorefinery cascade of *C. vulgaris* microalgae. *Foods* 11 (3), 471. https://doi.org/10.3390/foods11030471.

Chen, L.Y., Cheng, C.W., Liang, J.Y., 2015. Effect of esterification condensation on the Folin–Ciocalteu method for the quantitative measurement of total phenols. *Food Chem.* 170, 10–15. https://doi.org/10.1016/j.foodchem.2014.08.038.

Chovanček, E., Salazar, J., Şirin, S., Allahverdiyeva, Y., 2023. Microalgae from Nordic collections demonstrate biostimulant effect by enhancing plant growth and photosynthetic performance. *Physiol. Plant.* 175. https://doi.org/10.1111/ppl.13911.

du Jardin, P., Xu, L., Geelen, D., 2020. Agricultural functions and action mechanisms of plant biostimulants (PBs). In: Geelen, D., Xu, L. (Eds.), The Chemical Biology of Plant Biostimulants. John Wiley & Sons Ltd, UK, pp. 1–30.

Ferreira, A., Bastos, C.R.V., Marques-dos-Santos, C., Acién-Fernandez, F.G., Gouveia, L., 2023. Algaeculture for agriculture: From past to future. *Front. in Agron.* 5. https://doi.org/10.3389/fagro.2023.1064041.

French, K.E., Harvey, J., McCullagh, J.S.O., 2018. Targeted and untargeted metabolic profiling of wild grassland plants identifies antibiotic and anthelmintic compounds targeting pathogen physiology, metabolism and reproduction. *Scientif. Rep.* 8. https://doi.org/10.1038/s41598-018-20091-z.

Gemin, L.G., Mógor, Á.F., De Oliveira-Amatussi, J., Mógor, G., 2019. Microalgae associated to humic acid as a novel biostimulant improving onion growth and yield. *Scientia Hortic.* 256, 108560. https://doi.org/10.1016/j.scienta.2019.108560.

Hankamer, B., Pregelj, L., O'Kane, S., Hussey, K., Hine, D., 2023. Delivering impactful solutions for the bioeconomy. *Trends in Plant Sci.* 28, 583–596. https://doi.org/10.1016/j.tplants.2023.02.007.

Johnson, K.M., Sieburth, J.M., 1977. Dissolved carbohydrates in seawater. I, A precise spectrophotometric analysis for monosaccharides. *Marine Chem.* 5, 1–13. https://doi.org/10.1016/0304-4203(77)90011-1.

Jokel, M., Salazar, J., Chovancek, E., Sirin, S., Allahverdiyeva, Y., 2023. Screening of several microalgae revealed biopesticide properties of *Chlorella sorokiniana* against the strawberry pathogen *Phytophthora cactorum*. *J. of Appl. Phycol.* 35, 2675–2687. https://doi.org/10.1007/s10811-023-03015-x.

Kalita, P., Tapan, B.K., Pal, T.K., Kalita, R., 2013. Estimation of total flavonoids content (TFC) and antioxidant activities of methanolic whole plant extract of *Biophytum sensitivum* LINN. *J. of Drug Deliv. and Ther.* 3. https://doi.org/10.22270/jddt.v3i4.546.

Kapoore, R.V., Wood, E.E., Llewellyn, C.A., 2021. Algae biostimulants: A critical look at microalgal biostimulants for sustainable agricultural practices. *Biotechnol. Adv.* 49, 107754. https://doi.org/10.1016/j.biotechadv.2021.107754.

Liu, W., Feng, Y., Yu, S., Fan, Z., Li, X., Li, J., Yin, H., 2021. The flavonoid biosynthesis network in plants. *Int. J. of Mol. Sci.* 22, 12824. https://doi.org/10.3390/ijms222312824.

Mouillon, J.M., Aubert, S., Bourguignon, J., Gout, E., Douce, R., Rébeillé, F., 1999. Glycine and serine catabolism in non-photosynthetic higher plant cells: Their role in C1 metabolism. *The Plant J.* 20, 197–205. https://doi.org/10.1046/j.1365-313x.1999.00591.x.

Moyo, M., Ndhlala, A.R., Finnie, J.F., van Staden, J., 2010. Phenolic composition, antioxidant and acetylcholinesterase inhibitory activities of *Sclerocarya birrea* and *Harpephyllum caffrum* (Anacardiaceae) extracts. *Food Chem.* 123, 69–76. https://doi.org/10.1016/j.foodchem.2010.03.130.

Mutale-Joan, C., Redouane, B., Najib, E., Yassine, K., Lyamlouli, K., Laila, S., Zeroual, Y., El Arroussi, H., 2020. Screening of microalgae liquid extracts for their biostimulant properties on plant growth, nutrient uptake and metabolite profile of *Solanum lycopersicum* L. *Scientif. Rep.* 10. https://doi.org/10.1038/s41598-020-59840-4.

Navarro-López, E., Ruíz-Nieto, A., Ferreira, A., Acién, F.G., Gouveia, L., 2020. Biostimulant potential of Scenedesmus obliquus grown in brewery wastewater. *Molecules* 25 (3), 664. https://doi.org/10.3390/molecules25030664.

Neuberger, A., 1980. The regulation of chlorophyll and porphyrin biosynthesis. *Int. J. of Biochem.* 12, 787–789. https://doi.org/10.1016/0020-711x(80)90163-9.

Nielsen, P.M., Petersen, D., Dambmann, C., 2001. Improved method for determining food protein degree of hydrolysis. *J. of Food Sci.* 66, 642–646. https://doi.org/10.1111/j.1365-2621.2001.tb04614.x.

Nowak, A., Zagórska-Dziok, M., Ossowicz-Rupniewska, P., Makuch, E., Duchnik, W., Kucharski, Ł., Adamiak-Giera, U., et al., 2021. *Epilobium angustifolium* L. extracts as valuable ingredients in cosmetic and dermatological products. *Molecules* 26, 3456. https://doi.org/10.3390/molecules26113456.

Oancea, F., Velea, S., Fătu, V., Mincea, C., Ilie, L., 2013. Microalgae based plant biostimulant and its effect on water stressed tomato plants. Rom. J. of Plant Protection 6, 104–117.

Parmar, P., Kumar, R., Neha, Y., Srivatsan, V., 2023. Microalgae as next generation plant growth additives: Functions, applications, challenges and circular bioeconomy based solutions. *Front. in Plant Sci.* 14. https://doi.org/10.3389/fpls.2023.1073546.

Paul, K., Sorrentino, M., Lucini, L., Rouphael, Y., Cardarelli, M., Bonini, P., Begoña, M., Moreno, M., et al., 2019. A combined phenotypic and metabolomic approach for elucidating the biostimulant action of a plant-derived protein hydrolysate on tomato grown under limited water availability. *Front. in Plant Sci.* 10. https://doi.org/10.3389/fpls.2019.00493.

Premaratne, M., Nishshanka, G.K.S.H., Anthonio, R.A.D.P., Liyanaarachchi, V.C., Thevarajah, B., Nimarshana, P.H.V., Malik, A., Ariyadasa, T.U., 2022. Resource recovery from waste streams for production of microalgae biomass: A sustainable approach towards high-value biorefineries. *Bioresour. Technol. Rep.* 18, 101070. https://doi.org/10.1016/j.biteb.2022.101070.

Puglisi, I., La Bella, E., Rovetto, E.I., Stevanato, P., Fascella, G., Baglieri, A., 2022. Morpho-biometric and biochemical responses in lettuce seedlings treated by different application methods of *Chlorella vulgaris* extract: Foliar spray or root drench? *J. of Appl. Phycol.* 34, 889–901. https://doi.org/10.1007/s10811-021-02671-1.

Ramaroson, M.L., Koutouan, C., Helesbeux, J.J., Le Clerc, V., Hamama, L., Geoffriau, E., Briard, M., 2022. Role of phenylpropanoids and flavonoids in plant resistance to pests and diseases. *Molecules* 27 (23), 8371. https://doi.org/10.3390/molecules27238371.

Sakuraba, Y., 2022. Molecular basis of nitrogen starvation-induced leaf senescence. *Front. in Plant Sci.* 13. https://doi.org/10.3389/fpls.2022.1013304.

Santoro, D.F., Puglisi, I., Sicilia, A., Baglieri, A., La Bella, E., Lo Piero, A.R., 2023. Transcriptomic profile of lettuce seedlings (*Lactuca sativa*) response to microalgae extracts used as biostimulant agents. *AoB Plants* 15. https://doi.org/10.1093/aobpla/plad043.

Stirk, W.A., Bálint, P., Vambe, M., Lovász, C., Molnár, Z., van Staden, J., Ördög, V., 2020. Effect of cell disruption methods on the extraction of bioactive metabolites from microalgal biomass. *J. of Biotechnol.* 307, 35–43. https://doi.org/10.1016/j.jbiotec.2019.10.012.

Suleiman, A.K.A., Lourenço, K.S., Clark, C., Luz, R.L., da Silva, G.H.R., Vet, L.E., Cantarella, H., Fernandes, T.V., Kuramae, E.E., 2020. From toilet to agriculture: Fertilization with microalgal biomass from wastewater impacts the soil and rhizosphere active microbiomes, greenhouse gas emissions and plant growth. *Res., Conservation and Recycl.* 161, 104924. https://doi.org/10.1016/j.resconrec.2020.104924.

Thoday-Kennedy, E., Joshi, S., Daetwyler, H.D., Hayden, M., Hudson, D., Spangenberg, G., Kant, S., 2021. Digital phenotyping to delineate salinity response in safflower genotypes. *Front. in Plant Sci.* 12. https://doi.org/10.3389/fpls.2021.662498.

Tong, W.Y., 2013. Biotransformation of terpenoids and steroids. In: *Natural Products*. Springer, Berlin-Heidelberg, pp. 2733–2759. https://doi.org/10.1007/978-3-642-22144-6_122.

Tripathi, A., Pohanková, E., Fischer, M., Orság, M., Trnka, M., Klem, K., Marek, M., 2018. The evaluation of radiation use efficiency and leaf area index development for the estimation of biomass accumulation in short rotation poplar and annual field crops. *Forests* 9, 168. https://doi.org/10.3390/f9040168.

Tzin, V., Galili, G., 2010. New insights into the shikimate and aromatic amino acids biosynthesis pathways in plants. *Mol. Plant* 3, 956–972. https://doi.org/10.1093/mp/ssq048.

van der Rest, B., Boisson, A.M., Gout, E., Bligny, R., Douce, R., 2002. Glycerophosphocholine metabolism in higher plant cells: Evidence of a new glyceryl-phosphodiester phosphodiesterase. *Plant Physiol.* 130, 244–255. https://doi.org/10.1104/pp.003392.

Verified-Market. 2024. Biostimulants market size and forecast. *https://www.verifiedmarketresearch.com/product/biostimulants-market/* (accessed on 08-04-2024).

Windarsih, A., Suratno, Warmiko, H.D., Indrianingsih, A.W., Rohman, A., Ulumuddin, Y. I. 2022. Untargeted metabolomics and proteomics approach using liquid chromatography-Orbitrap high resolution mass spectrometry to detect pork

adulteration in *Pangasius hypopthalmus* meat. *Food Chem.* 386, 132856. doi: 10.1016/j.foodchem.2022.132856.

Yun, J.H., Nam, J.W., Yang, J.H., Lee, Y.J., Cho, D.H., Choi, H.I., Hong, J.S., Ahn, K.H., Kim, H.S. 2024. Toward a zero-waste microalgal biorefinery: Complete utilization of defatted Chlorella biomass as a sole heterotrophic substrate for Chlorella sp. HS2 and an improved composite filler. Chem. Engineering J., 480,147998. doi.org/10.1016/j.cej.2023.147998.

Zhang, Y., Guo, S., Xie, C., Fang, J., 2020. Uridine metabolism and its role in glucose, lipid, and amino acid homeostasis. *BioMed Res. Int.* 2020, 1–7. https://doi.org/10.1155/2020/7091718.